Increased signal intensity of the cochlea on pre- and post-contrast enhanced 3D-FLAIR in patients with vestibular schwannoma

Masahiro Yamazaki, Shinji Naganawa, Hisashi Kawai, Takashi Nihashi

Department of Radiology, Nagoya University Graduate School of Medicine, Nagoya, Japan

Hiroshi Fukatsu

Department of Medical Informatics, Aichi Medical University Hospital, Nagakute, Japan

Tsutomu Nakashima

Department of Otorhinolaryngology, Nagoya University Graduate School of Medicine, Nagoya, Japan

Address for correspondence
Masahiro Yamazaki, MD
Department of Radiology,
Nagoya University Graduate School of Medicine,
65 Tsurumai-cho, Showa-ku,
Nagoya, 466-8550,
Japan.
Telephone: +81-52-7442327
Fax: +81-52-7442335
E-mail: yamazaki@med.nagoya-u.ac.jp

Abstract

Introduction: In the vestibular schwannoma patients, the pathophysiologic mechanism of inner ear involvement is still unclear. We investigated the status of the cochleae in patients with vestibular schwannoma by evaluating the signal intensity of cochlear fluid on pre- and post-contrast enhanced thin section three-dimensional fluid attenuated inversion recovery (3D-FLAIR).

Methods: Twenty-eight patients were retrospectively analyzed. Post-contrast images were obtained in 18 patients and 20 patients had the records of their pure-tone audiometry. Regions of interest of both cochleae (C) and of the medulla oblongata (M) were determined on 3D-FLAIR images by referring to 3D-heavily T2-weighted images on a workstation. The signal intensity ratio between C and M on the 3D-FLAIR images (CM ratio) was then evaluated. In addition, correlation between the CM ratio and the hearing level was also evaluated.

Results: The CM ratio of the affected side was significantly higher than that of the unaffected side ($p<0.001$). In the affected side, post-contrast signal elevation was observed ($p<0.005$). In 13 patients (26 cochleae) who underwent both gadolinium injection and the pure-tone audiometry, the post-contrast CM ratio correlated with hearing level ($p<0.05$).

Conclusion: The results of present study suggest that alteration of cochlear fluid composition and increased permeability of the blood-labyrinthine barrier exist in the affected side in patients with vestibular schwannoma. Furthermore, although weak, positive correlation between post-contrast cochlear signal intensity on 3D-FLAIR and hearing level warrants further study to clarify the relationship between 3D-FLAIR findings and prognosis of hearing preservation surgery.

Keywords: magnetic resonance, FLAIR, high resolution, vestibular schwannoma, cochlea

Increased signal intensity of the cochlea on pre- and post-contrast enhanced 3D-FLAIR in patients with vestibular schwannoma

Introduction

In patients with vestibular schwannoma, presenting complaints are unilateral hearing reduction or an episode of sudden hearing loss, although the pathophysiologic mechanism of inner ear involvement is still unclear. In past reports, Silverstein et al. suggested protein level elevation of cochlear perilymph in patients with vestibular schwannoma who underwent the labyrinthine tap as the diagnostic test [1–4]. However, the labyrinthine tap has since been completely abandoned due to the risk of causing deafness. Currently, CT or MR imaging are the differential diagnosis tools of choice in patients with hearing loss. Therefore, investigation into cochlear protein levels have necessarily been suspended for the time being.

CT is indicated to assess conduction hearing deficit while MR is the procedure of choice for sensorineural hearing loss. FLAIR (fluid attenuated inversion recovery) imaging is sensitive in detecting high protein contents in fluids such as cerebrospinal fluid and various cystic intracranial mass lesions [5, 6]. Three-dimensional FLAIR (3D-FLAIR) images can minimize the undesired inflow ghosts of cerebrospinal fluid flow [7], and enable recognition of the subtle compositional changes in lymph fluid in the inner ear that cannot be detected by T1-weighted images [8–10]. Furthermore, increased permeability of the blood-labyrinthine barrier can also be observed on post-contrast 3D-FLAIR images; this technique has been reported to be useful for pathophysiologic analysis of the inner ear in many auditory diseases such as sudden sensorineural hearing loss, cholesteatoma and cochlear otosclerosis [11–13].

The purposes of the present study were to evaluate the signal intensity of cochlear fluid on pre- and post-contrast-enhanced thin sections by 3D-FLAIR in patients with

vestibular schwannoma, and to investigate the relationship between auditory function and signal alteration.

Materials and methods

Study population

This study was approved by the Ethics Review Committee of our institution (approval number 729). The requirement for informed patient consent was waived owing to the retrospective nature of the study. The records of 28 patients (10 males and 18 females; mean age, 62 years; range, 12–79 years) with unilateral vestibular schwannoma who underwent the MR imaging of the inner ear including 3D-FLAIR sequence at our hospital from January 2007 to June 2008 were retrospectively examined. All of the patients had been diagnosed on the basis of typical MR imaging appearances by an experienced neuroradiologist (S. N.). In this patient group, there was no bilateral case, neurofibromatosis type 2 or intracochlear lesion. Two patients underwent surgical treatment and one patient received gamma knife radiosurgery after diagnosis. The remaining 25 patients were followed without aggressive medical treatments such as surgical treatment and gamma knife radiosurgery. Three patients had a history of gamma knife radiosurgery before coming to our hospital. Eighteen patients also had pre- and post-contrast MR imaging of the inner ear by intravenous administration of gadolinium-diethylene-triamine pentaacetic acid (Gd-DTPA; Magnevist, Bayer Yakuhin, Ltd., Osaka, Japan) or gadolinium-diethylene-triamine pentaacetic acid-bis (methylamide) (Gd-DTPA-BMA; Omniscan, Daiichi Sankyo Co., Ltd., Tokyo, Japan). Twenty patients had the records of their pure-tone audiometry data within a month of the MR examination. In other eight patients, it was impossible to obtain pure-tone

audiometry data around the MR examination because some referred from other hospitals for MR imaging, others had longer interval from pure-tone audiometry to the MR examination. Thirteen patients underwent both gadolinium injection and the pure-tone audiometry.

MR imaging protocol

All patients underwent axial 3D-FLAIR, 3D-T1-weighted imaging (T1WI) and 3D-heavily T2-weighted imaging (T2WI) of the inner ear. Images were obtained on whichever 3T scanner (MAGNETOM Trio; Siemens AG, Erlangen, Germany) or on two types of 1.5T scanners (MAGNETOM Avanto; Siemens AG, Erlangen, Germany or EXCELART Vantage; Toshiba, Tokyo, Japan) using a receive-only, 12-channel (on Siemens Trio, Avanto) or 10-channel (on Toshiba Vantage), phased-array coil. Ten patients obtained MR imaging on Trio scanner, 12 patients on Avanto scanner, and 6 patients on Vantage scanner. Eighteen patients had 3D-FLAIR and 3D-T1WI after intravenous gadolinium contrast agent administration (Gd-DTPA or Gd-DTPA-BMA; 0.1 mmol/kg body weight in total amount). After the contrast was administered, 3D-T1WI was scanned first. Then post-contrast 3D-FLAIR was initiated 7 minutes after the gadolinium was administered so that the contrast of 3D-FLAIR was determined approximately 10 minutes after the administration of gadolinium. The slice thickness of all images was 0.8 mm.

The sequence parameters for 3D-FLAIR, 3D-T1WI and 3D-heavily T2WI are shown in Table 1. 3D-T1WI were obtained using a spoiled gradient echo sequence. 3D-heavily T2WI were obtained using a gradient echo based sequence on a 3T scanner and a spin echo based sequence on 1.5T scanners.

MR imaging analysis

Image analysis was performed on a picture archiving and communication system (PACS) workstation. In each patient, regions of interest (ROI) of both cochleae and of the medulla oblongata were determined on 3D-FLAIR images by referring to 3D-heavily T2WI at a workstation (Figure 1). The ROI were drawn around each cochlea on the 3D-heavily T2WI at the level of the modiolus. Similarly, a ROI was drawn around the medulla oblongata on 3D-heavily T2WI. Then they were copied onto identical slices of 3D-FLAIR images, which provided the ROIs for the 3D-FLAIR images. The ratio of cochlear signal intensity to that of the medulla oblongata (CM ratio) on the 3D-FLAIR images was determined for each cochlea. In a manner similar to 3D-FLAIR imaging, the CM ratio on 3D-T1WI was determined. The CM ratio was calculated in both pre-contrast and in post-contrast 3D-FLAIR and 3D-T1WI. The reason for selecting the medulla oblongata as the reference for calculating the CM ratio was to compare the cochlear signal intensity of affected side with that of unaffected side statistically. Tumors were classified into two groups, based on the presence or absence of extension to the cochlear area at the fundus of the internal auditory canal (IAC). The maximal linear diameters of the tumors were also measured on 3D-heavily T2WI. These measurements were performed by one radiologist (M.Y.) who did have prior knowledge of the existence of vestibular schwannoma. Measuring the signal in a blinded manner was not feasible in this study.

Audiological assessment

Hearing levels were evaluated using an audiometer (Model AA-79S; Rion, Tokyo, Japan) in a sound-insulated chamber. If the patient did not respond to the maximum

sound level produced by the audiometer, we defined the threshold as 5 dB added to the maximum level. The average hearing level was calculated as the mean of the hearing levels measured at 500, 1,000, 2,000, and 3,000 Hz on the basis of the American Academy of Otolaryngology-Head and Neck Surgery guidelines in vestibular schwannoma [14].

Statistical analysis

Differences in CM ratio between the affected and unaffected sides, between pre- and post-contrast, and the hearing level difference between affected and unaffected sides were compared using a paired *t*-test. The differences in CM ratio between the affected and unaffected sides were assessed in both pre-contrast and in post-contrast 3D-FLAIR and 3D-T1WI. Student's *t*-test was used to compare the CM ratio on pre-contrast 3D-FLAIR images on the affected side between the groups with or without invasion of the fundus of the IAC. Differences in CM ratio of the affected side between 3T scanner and 1.5T scanners on both 3D-FLAIR and 3D-T1WI were compared also using Student's *t*-test. The relationship between the CM ratio on pre-contrast 3D-FLAIR and tumor diameter was investigated using Pearson's correlation coefficient test. The relationship between the CM ratio on both pre- and post-contrast 3D-FLAIR images and hearing level was investigated using Spearman's correlation coefficient by rank test. In our statistical analysis, a value of $p<0.05$ represented statistical significance.

Results

Fourteen of the 28 tumors had extension to the cochlear area at the fundus of the IAC while the other 14 did not. The mean size of the vestibular schwannomas was 10.0 mm (range, 2.8–21.5 mm).

None of the patients showed a visible abnormality of medulla oblongata on all images and high signal of cochlea that would have suggested hemorrhage on pre-contrast 3D-T1WI. There was no significant difference between the affected side and unaffected side CM ratio on pre-contrast 3D-T1WI (the mean CM ratio was 0.46±0.07 on affected side, 0.46±0.07 on unaffected side, $p=0.93$). The mean CM ratio on the pre-contrast 3D-FLAIR images for the affected side was 0.59±0.18, while that for the unaffected side was 0.33±0.10 ($p<0.001$, Figure 2). There was no significant difference in CM ratio on pre-contrast 3D-FLAIR and 3D-T1WI on the affected side between 3T scanner (the mean CM ratio was 0.68±0.12 on 3D-FLAIR, 0.44±0.06 on 3D-T1WI) and 1.5T scanners (the mean CM ratio was 0.54±0.19 on 3D-FLAIR, 0.47±0.08 on 3D-T1WI) ($p=0.06$ on 3D-FLAIR, $p=0.20$ on 3D-T1WI). In addition, there was no significant difference in CM ratio on pre-contrast 3D-FLAIR images of the affected side between tumors with extension to the cochlear area at the fundus of the IAC (the mean CM ratio was 0.63±0.13) and those without extension (the mean CM ratio was 0.55±0.22) ($p=0.28$). Furthermore, there was no significant correlation between tumor diameter and CM ratio on pre-contrast 3D-FLAIR images ($r=0.37$, $p=0.05$).

In the 18 patients who had post-contrast imaging of the inner ear, the mean CM ratio on the post-contrast 3D-FLAIR images for the affected side was 0.74±0.15, while that for the unaffected side was 0.35±0.12 ($p<0.001$, Figure 3). There was no significant difference between the affected side and unaffected side CM ratio on post-contrast

3D-T1WI (the mean CM ratio was 0.46±0.08 on affected side, 0.44±0.07 on unaffected side, p=0.26). In the affected side of the 18 patients who had post-contrast imaging of the inner ear, the mean CM ratio on pre-contrast 3D-FLAIR images was 0.66±0.13, while that for the post-contrast images was 0.74±0.15 ($p<0.005$). There was no significant difference between pre- and post-contrast CM ratio on 3D-T1WI of the affected side (the mean CM ratio was 0.45±0.08 on pre-contrast, 0.45±0.07 on post-contrast, p=0.60). There was no significant difference in CM ratio on post-contrast 3D-FLAIR and 3D-T1WI on the affected side between 3T scanner (the mean CM ratio was 0.80±0.13 on 3D-FLAIR, 0.45±0.07 on 3D-T1WI) and 1.5T scanners (the mean CM ratio was 0.68±0.15 on 3D-FLAIR, 0.46±0.09 on 3D-T1WI) (p=0.09 on 3D-FLAIR, p=0.75 on 3D-T1WI). In the unaffected side, there were no significant differences between pre- and post-contrast CM ratio on both 3D-FLAIR (the mean CM ratio was 0.33±0.11 on pre-contrast, 0.35±0.12 on post-contrast, p=0.88) and 3D-T1WI (the mean CM ratio was 0.46±0.07 on pre-contrast, 0.44±0.07 on post-contrast, p=0.21).

In the 20 patients who underwent a pure-tone audiometry, the mean hearing level for the affected side was 53.2±33.2 dB, while that for the unaffected side was 22.7±14.3 dB ($p<0.001$). When we limit the evaluation only on affected side, Spearman's correlation coefficient by rank test showed no significant correlation between both pre- and post-contrast CM ratio on 3D-FLAIR images and hearing level (pre-contrast: n=20, r=0.06; post-contrast: n=13, r=-0.02). Meanwhile, provided affected side and unaffected side were assessed together, there was no significant correlation between pre-contrast CM ratio on 3D-FLAIR images and hearing level (n=40, r=0.27, p=0.09), although the CM ratio on post-contrast 3D-FLAIR images correlated with hearing level (n=26, r=0.47, $p<0.05$, Figure 4).

Discussion

The results of the present study suggest alteration of cochlear fluid composition in the affected side of patients with vestibular schwannoma. This is consistent with previous studies using the surgical approach [1–4, 15–17]. MR imaging using the 3D-FLAIR technique makes it possible to determine the condition of the inner ear lymph fluid without cerebrospinal fluid inflow and pulsation artifacts or invasive surgical procedures, which carry some risk of contamination of the perilymph with blood and other fluids. On 3D-T1WI, changes in inner ear lymph fluid composition cannot be recognized.

We also observed post-contrast signal elevation on the affected side. Usually on 3D-FLAIR images, enhancement of the cochlear fluid cannot be detected at 10 minutes after gadolinium injection [18]. Therefore, this result suggests increased permeability of the blood-labyrinthine barrier in the affected side. On the other hand, there was no significant difference between pre- and post-contrast CM ratio on 3D-T1WI. The contrast effect on FLAIR is reported to be higher than T1WI at the concentration of extravasated gadolinium below 0.7 mmol/L [19, 20]. It is more than probable that the leakage of gadolinium contrast agent to cochlear fluid is too low concentration to recognize on T1WI. Furthermore, provided affected side and unaffected side were assessed together, correlation between the post-contrast CM ratio on 3D-FLAIR images and the degree of hearing impairment was suggested, although no correlation was observed between the pre-contrast CM ratio and hearing level. Thus it appears that in patients with vestibular schwannoma, increased permeability of the blood-labyrinthine barrier in the cochlea may be one of the important causes of hearing loss, as seen in

cases of meningitis, and noise-induced and sensorineural hearing loss [21–23]. However, when we evaluate only on affected side, there was no significant correlation between CM ratio on 3D-FLAIR images and hearing level. This result possibly to be caused by small number of patients, further accumulation of cases and additional evaluation are necessary. Additionally, although the correlation between tumor diameter and CM ratio on pre-contrast 3D-FLAIR images did not reach significance ($p=0.05$), the r value obtained 0.37 likely indicates that the reason for this result is the small number of patients included.

The protein level elevation of cochlear perilymph in patients with vestibular schwannoma was reported in past times, and the origin of the elevated protein was discussed in many studies [1-4, 15-17, 24-27]. There are three main hypotheses that explain the cause of increased cochlear perilymph protein level in patients with vestibular schwannoma. These are cochlear membrane damage by blood vessel stasis either in artery or vein resulting in increased permeability [2, 16, 24], neuroaxonal protein transport blockage in the cochlear nerve caused by tumor compression [17], and cell-mediated immune reaction in the inner ear to antigenic properties of vestibular schwannomas [26, 27]. Each pattern could cause perilymph protein increase. However, a vascular disorder, more specifically increased permeability of the blood-labyrinthine barrier, might also be closely related to the degree of hearing loss in patients with vestibular schwannoma, based on the present study.

Yoshida et al. reported that cochlear signal intensity on 3D-FLAIR images in patients with sudden sensorineural hearing loss (SNHL) was increased in many cases and that a high signal in the cochlea on pre-contrast 3D-FLAIR images is related to a poor hearing

prognosis, although they found no relationship between cochlear signal intensity and initial hearing level [28]. Meanwhile, hearing improvement in patients who showed post-contrast enhancement on 3D-FLAIR images in the affected inner ear was not significantly different from that in patients who did not. Although the pathology of SNHL remains unclear, vascular compromise and immunologic diseases have been hypothesized [29, 30], which might have something in common with the pathological hypotheses in vestibular schwannoma. Thus, pre-contrast cochlear signal intensity on 3D-FLAIR images might be a prognostic factor in patients with vestibular schwannoma. In addition, cochlear post-contrast 3D-FLAIR signal intensity has the potential for correlation with initial hearing level in patients with sudden sensorineural hearing loss.

The 3D-FLAIR technique can provide high resolution images [31, 32]. In addition, FLAIR images are sensitive in detecting a high protein content of fluid [5, 6]. It is conceivable that a signal decrease on CISS images, which reflects liquid T2/T1 lowering, can indicate the existence of hemorrhage and/or a high protein content of fluid [33, 34]. However, in past reports, most signal changes observed on 3D-FLAIR images could not be detected on CISS images [28, 35, 36]. Consequently, 3D-FLAIR images appear more sensitive in detecting a high protein content of fluid than CISS images. Furthermore, because signal changes in CISS images are represented as loss of intensity, it is difficult to completely avoid the influence of magnetic susceptibility artifacts and the partial volume effect [37]. Therefore, we applied 3D-FLAIR in the current investigation to evaluate cochlear fluid composition changes in patients with vestibular schwannoma.

Somers et al. reported that intra-labyrinthine signal intensity on CISS images should be a valuable tool for determining candidacy for hearing preservation surgery [34]. When a cochlear signal intensity decrease is detected on CISS images, it is conceivable that a relatively strong composition change may arise in the lymph fluid. On the other hand, 3D-FLAIR images would be so sensitive in detecting the protein content of fluid that faint and reversible alterations in lymph fluid composition could be detected. Consequently, in the future, quantitative analysis of cochlear signal intensity using 3D-FLAIR images may be a prognostic indicator of hearing preservation surgery.

Recently, Bhadelia et al. reported a cochlear FLAIR signal increase in patients with vestibular schwannoma using 5 mm section thickness, two-dimensional pre-contrast FLAIR imaging [38]. They were able to place ROI within the cochlea without difficulty because the cochlea was markedly hyperintense on the affected side, although evaluation of the unaffected side and control subjects was difficult due to the small size of the cochlea. In our study, 0.8 mm thick high resolution isotropic 3D-FLAIR imaging was used and the ROI were set with accuracy by referring to 3D-heavily T2WI. On the other hand, our study has some limitations, in that our retrospective study collected data from images taken by multiple MR scanners, group of patients was heterogenous and signal intensity measurement was semiquantitative without using external phantoms for reference.

In conclusion, the results of the present study suggest that alteration of cochlear fluid composition and increased permeability of the blood-labyrinthine barrier are present in the affected side in patients with vestibular schwannoma. Furthermore, we found, although weak, positive correlation between post-contrast cochlear signal intensity on

3D-FLAIR images and the degree of hearing impairment. These results suggest that alteration of perilymph composition might be responsible for inner ear disorders in patients with vestibular schwannoma and that increased permeability of the blood-labyrinthine barrier might be closely related to the degree of hearing loss. These results warrant the further study to clarify the relationship between 3D-FLAIR findings and prognosis of hearing preservation surgery.

Figure Legends

Figure 1

A 3D-CISS image and a 3D-FLAIR image at the level of the modiolus (a, b) and a 3D-FLAIR image at the level of the medulla oblongata (c) of a 36-year-old man with vestibular schwannoma in his right internal auditory canal (IAC) are presented. Vestibular schwannoma was detected in the IAC (arrows on a, b). The ROI of the cochlea were determined on 3D-FLAIR images by referring to 3D-heavily T2WI at a workstation. The ROI were drawn around each cochlea on the 3D-heavily T2WI at the level of the modiolus (a), then they were copied onto identical slices of 3D-FLAIR images (b), which provided the ROIs for 3D-FLAIR imaging. The ROIs of the medulla oblongata on 3D-FLAIR images were similarly set (c).

Figure 2

Bilateral 3D-CISS images (a, b) and pre-contrast 3D-FLAIR images (c, d) at the level of the modiolus of a 49-year-old man with vestibular schwannoma in his right internal auditory canal (arrows on a, c) are presented. A right cochlear signal intensity increase is seen on the 3D-FLAIR image (arrowhead on c). On the other hand, the left cochlear

signal intensity on the 3D-FLAIR image is very faint and it has ill-defined borders. On 3D-CISS images, cochlear signal intensity difference between both sides is not so obvious as 3D-FLAIR.

Figure 3

Bilateral 3D-CISS images (a, b), pre- (c, d) and post-contrast (e, f) 3D-T1WI, and pre- (g, h) and post-contrast (i, j) 3D-FLAIR images at the level of the modiolus of a 55-year-old woman with vestibular schwannoma in her left internal auditory canal (IAC, arrow on b, f) are presented. On the 3D-T1WI, there is no signal difference between both cochleae and no signal elevation is observed after gadolinium injection. In contrast, on the pre-contrast 3D-FLAIR image, the left cochlear signal intensity increase is seen (arrowhead on h). On the post-contrast 3D-FLAIR image, further signal elevation of the left cochlea can be observed (arrowhead on j). In addition, leakage of gadolinium agent is seen at the fundus of the left IAC (arrow on j).

Figure 4

In all 13 patients (26 ears) who underwent both gadolinium injection and a pure-tone audiometry, the post-contrast CM ratio on 3D-FLAIR correlated with hearing level ($r=0.47$, $p<0.05$).

Conflict of interest statement

We declare that we have no conflict of interest.

References

1. Silverstein H, Schuknecht HF (1966) Biochemical studies of inner ear fluid in man: changes in otosclerosis, Meniere's disease, and acoustic neuroma. Arch Otolaryngol 84: 395–402

2. Silverstein H (1971) Inner ear fluid proteins in acoustic neuroma, Meniere's disease, and otosclerosis. Ann Otol Rhinol Laryngol 80: 27–35

3. Silverstein H (1973) Labyrinthine tap as a diagnostic test for acoustic neuroma. Otolaryngol Clin North Am 6: 229–244

4. Silverstein H, Naufal P, Belal A (1973) Causes of elevated perilymph protein concentrations. Laryngoscope 83: 476–487

5. Melhem ER, Jara H, Eustace S (1997) Fluid-attenuated inversion recovery MR imaging: identification of protein concentration threshold for CSF hyperintensity. AJR Am J Roentgenol 169: 859–862

6. Mishra AM, Reddy SJ, Husain M, Behari S, Husain N, Prasad KN, Kumar S, Gupta RK (2006) Comparison of the magnetization transfer ratio and fluid-attenuated

inversion recovery imaging signal intensity in differentiation of various cystic intracranial mass lesions and its correlation with biological parameters. J Magn Reson Imaging 24: 52–56

7. Naganawa S, Koshikawa T, Nakamura T, Kawai H, Fukatsu H, Ishigaki T, Komada T, Maruyama K, Takizawa O (2004) Comparison of flow artifacts between 2D-FLAIR and 3D-FLAIR sequences at 3T. Eur Radiol 14: 1901–1908

8. Sugiura M, Naganawa S, Sato E, Nakashima T (2006) Visualization of a high protein concentration in the cochlea of a patient with a large endolymphatic duct and sac, using three-dimensional fluid-attenuated inversion recovery magnetic resonance imaging. J Laryngol Otol 120: 1084–1086

9. Sugiura M, Naganawa S, Teranishi M, Sato E, Kojima S, Nakashima T (2006) Inner ear hemorrhage in systemic lupus erythematosus. Laryngoscope 116: 826–828

10. Otake H, Sugiura M, Naganawa S, Nakashima T (2006) 3D-FLAIR magnetic resonance imaging in the evaluation of mumps deafness. Int J Pediatr Otorhinolaryngol 70: 2115–2117

11. Sugiura M, Naganawa S, Teranishi M, Nakashima T (2006) Three-dimensional fluid-attenuated inversion recovery magnetic resonance imaging findings in patients with sudden sensorineural hearing loss. Laryngoscope 116: 1451–1454

12. Sone M, Mizuno T, Sugiura M, Naganawa S, Nakashima T (2007) Three-dimensional fluid-attenuated inversion recovery magnetic resonance imaging investigation of inner ear disturbances in cases of middle ear cholesteatoma with labyrinthine fistula. Otol Neurotol 28: 1029–1033

13. Sugiura M, Naganawa S, Sone M, Yoshida T, Nakashima T (2008) Three-dimensional fluid attenuated inversion recovery magnetic resonance imaging findings in a patient with cochlear otosclerosis. Auris Nasus Larynx 35: 269–272

14. Committee on Hearing and Equilibrium, American Academy of Otolaryngology-Head and Neck Surgery (1995) Committee on Hearing and Equilibrium guidelines for the evaluation of hearing preservation in acoustic neuroma (vestibular schwannoma). Otolaryngol Head Neck Surg 113: 179–180

15. Eckermeier L, Pirsig W, Mueller D (1979) Histopathology of 30 non-operated acoustic schwannomas. Arch otorhinolaryngol 222: 1–9

16. O'Connor AF, France MW, Morrison AW (1981) Perilymph total protein levels associated with cerebellopontine angle lesions. Am J Otol 2: 193–195

17. Thomsen J, Saxtrup O, Tos M (1982) Quantitated determination of proteins in perilymph in patients with acoustic neuroma. ORL J Otorhinolaryngol Relat Spec 44: 61–65

18. Naganawa S, Komada T, Fukatsu H, Ishigaki T, Takizawa O (2006) Observation of contrast enhancement in the cochlear fluid space of healthy subjects using a 3D-FLAIR sequence at 3 Tesla. Eur Radiol 16: 733–737

19. Mathews VP, Caldemeyer KS, Lowe MJ, Greenspan SL, Weber DM, Ulmer JL (1999) Brain: gadolinium-enhanced fast fluid-attenuated inversion-recovery MR imaging. Radiology 211: 257–263

20. Jackson EF, Hayman LA (2000) Meningeal enhancement on fast FLAIR images. Radiology 215: 922–924

21. Kastenbauer S, Klein M, Koedel U, Pfister HW (2001) Reactive nitrogen species contribute to blood-labyrinth barrier disruption in suppurative labyrinthitis complicating experimental pneumococcal meningitis in the rat. Brain res 904: 208–217

22. Nakashima T, Naganawa S, Sone M, Tominaga M, Hayashi H, Yamamoto H, Liu X, Nuttall AL (2003) Disorders of cochlear blood flow. Brain Res Brain Res Rev 43: 17–28

23. Naganawa S, Sugiura M, Kawamura M, Fukatsu H, Nakashima T, Maruyama K (2006) Prompt contrast enhancement of cerebrospinal fluid space in the fundus of the internal auditory canal: Observations in patients with meningeal diseases on 3D-FLAIR images at 3 Tesla. Magn Reson Med Sci 5: 151–155

24. O'Connor AF, Luxon LM, Shortman RC, Thompson EJ, Morrison AW (1982) Electrophoretic separation and identification of perilymph proteins in cases of acoustic neuroma. Acta Otolaryngol 93: 195–200

25. Palva T, Raunio V (1982) Cerebrospinal fluid and acoustic neuroma specific proteins in perilymph. Acta Otolaryngol 93: 201–203

26. Rasmussen N, Bendtzen K, Thomsen J, Tos M (1983) Specific cellular immunity in acoustic neuroma patients. Otolaryngol Head Neck Surg 91: 532–536

27. Rasmussen N, Bendtzen K, Thomsen J, Tos M (1984) Antigenicity and protein content of perilymph in acoustic neuroma patients. Acta Otolaryngol 97: 502–508

28. Yoshida T, Sugiura M, Naganawa S, Teranishi M, Nakata S, Nakashima T (2008) Three-dimensional fluid-attenuated inversion recovery magnetic resonance imaging findings and prognosis in sudden sensorineural hearing loss. Laryngoscope 118: 1433–1437

29. Gussen R (1976) Sudden deafness of vascular origin: a human temporal bone study. Ann Otol Rhinol Laryngol 85: 94–100

30. Fitzgerald DC, Mark AS (1999) Viral cochleitis with gadolinium enhancement of the cochlea on magnetic resonance imaging scan. Otolaryngol Head Neck Surg 121: 130–132

31. Barker GJ (1998) 3D fast FLAIR: A CSF-nulled 3D fast spin-echo pulse sequence. Magn Reson Imaging 16: 715–720

32. Naganawa S, Kawai H, Fukatsu H, Ishigaki T, Komada T, Maruyama K, Takizawa O (2004) High-speed imaging at 3 Tesla: A technical and clinical review with an emphasis on whole-brain 3D imaging. Magn Reson Med Sci 3: 177–187

33. Haacke EM, Frahm J (1991) A guide to understanding key aspects of fast gradient-echo imaging. J Magn Reson Imaging 1: 621–624

34. Somers T, Casselman J, de Ceulaer G, Govaerts P, Offeciers E (2001) Prognostic value of magnetic resonance imaging findings in hearing preservation surgery for vestibular schwannoma. Otol Neurotol 22: 87–94

35. Naganawa S, Satake H, Kawamura M, Fukatsu H, Sone M, Nakashima T (2008) Separate visualization of endolymphatic space, perilymphatic space and bone by a single pulse sequence; 3D-inversion recovery imaging utilizing real reconstruction after intratympanic Gd-DTPA administration at 3 Tesla. Eur Radiol 18: 920–924

36. Naganawa S, Satake H, Iwano S, Fukatsu H, Sone M, Nakashima T (2008) Imaging endolymphatic hydrops at 3 Tesla using 3D-FLAIR with intratympanic Gd-DTPA administration. Magn Reson Med Sci 7: 85–91

37. Naganawa S, Koshikawa T, Fukatsu H, Ishigaki T, Fukuta T (2001) MR cisternography of the cerebellopontine angle: Comparison of three-dimensional fast asymmetrical spin-echo and three-dimensional constructive interference in the steady-state sequences. AJNR Am J Neuroradiol 22: 1179–1185

38. Bhadelia RA, Tedesco KL, Hwang S, Erbay SH, Lee PH, Shao W, Heilman C (2008) Increased cochlear fluid-attenuated inversion recovery signal in patients with vestibular schwannoma. AJNR Am J Neuroradiol 29: 720–723

Table 1

Table 1 MR sequence parameters

3D-FLAIR sequence parameters

	Scanner		
	3T (Siemens Trio)	1.5 (Siemens Avanto)	1.5T (Toshiba Vantage)
Repetition time (ms)	9000	8000	9000
Echo time (ms)	458 or 638	295 or 316 or 339	80
Inversion time (ms)	2500	2300	2500
Reconstructed voxel size (mm^3)	0.7 × 0.7 × 0.8	0.8 × 0.8 × 0.8	0.7 × 0.7 × 0.8
Echo train length	119 or 171	141	68
Echo space (ms)	3.7	4.3 or 4.6	6.5 or 10
Parallel factor	2 [a]	2 [a]	2 [b]
Pulse sequence	SPACE	SPACE	FASE
Scan time (minutes' seconds")	5' 26"	6' 26"	6' 45"

3D-T1 weighted imaging sequence parameters

	Scanner		
	3T (Siemens Trio)	1.5 (Siemens Avanto)	1.5T (Toshiba Vantage)
Repetition time (ms)	6.9 or 7.7	8.4 or 9.3 or 9.7	23.0
Echo time (ms)	3.3	3.5 or 3.6 or 3.9 or 4.4 or 4.6	5.5
Reconstructed voxel size (mm^3)	0.6 × 0.6 × 0.8	0.8 × 0.6 × 0.8	0.7 × 0.7 × 0.8 or 0.8 × 0.7 × 0.8 or 0.8 × 0.8 × 0.8
Parallel factor	2 [a]	2 [a]	1
Pulse sequence	VIBE	VIBE	SPGR
Scan time (minutes' seconds")	3' 49" or 4' 16"	3' 31" or 3' 52" or 4' 02"	3' 47"

3D-heavily T2 weighted imaging sequence parameters

	Scanner		
	3T (Siemens Trio)	1.5 (Siemens Avanto)	1.5T (Toshiba Vantage)
Repetition time (ms)	6.4 or 8.8	1200	4000
Echo time (ms)	3.2 or 4.4	262 or 264	240 or 300
Reconstructed voxel size (mm^3)	$0.5 \times 0.5 \times 0.8$	$0.8 \times 0.6 \times 0.8$	$0.6 \times 0.3 \times 0.8$ or $0.6 \times 0.4 \times 0.8$
Echo train length	-	71	72
Echo space (ms)	-	5.7 or 6.1	15
Parallel factor	2 [a]	2 [a]	1
Pulse sequence	CISS	SPACE	FASE
Scan time (minutes' seconds")	3' 15" or 5' 13"	4' 21"	5' 56"

[a] GRAPPA: Generalized autocalibrating partially parallel acquisition

[b] SPEEDER: A kind of SENSE (Sensitivity encoding)

SPACE: Sampling perfection with application optimized contrast using different flip angle evolutions

FASE: Fast asymmetric spin echo

VIBE: Volumetric interpolated breath hold examination

SPGR: Spoiled gradient recalled acquisition in the steady state

CISS: Constructive interference in the steady state

Figure 1

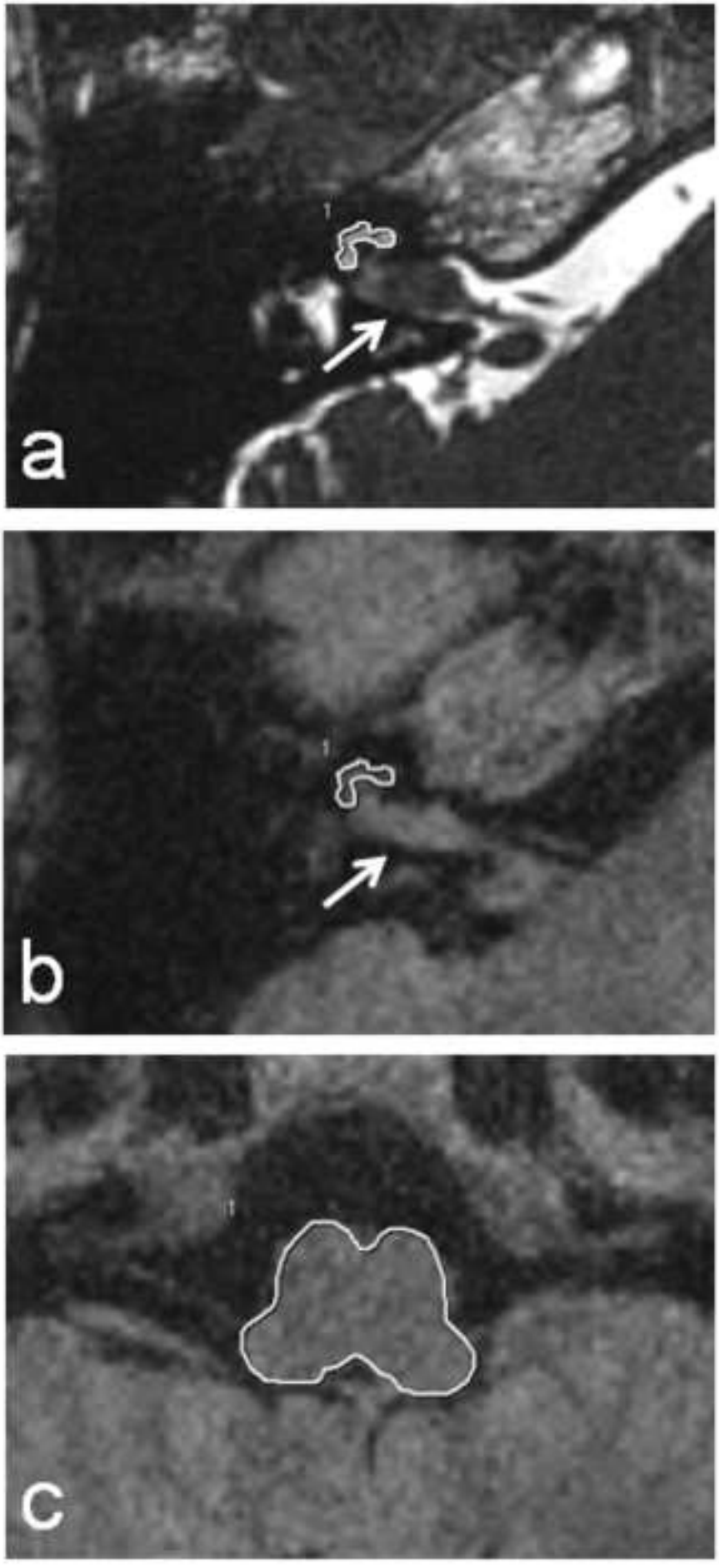

Figure 2

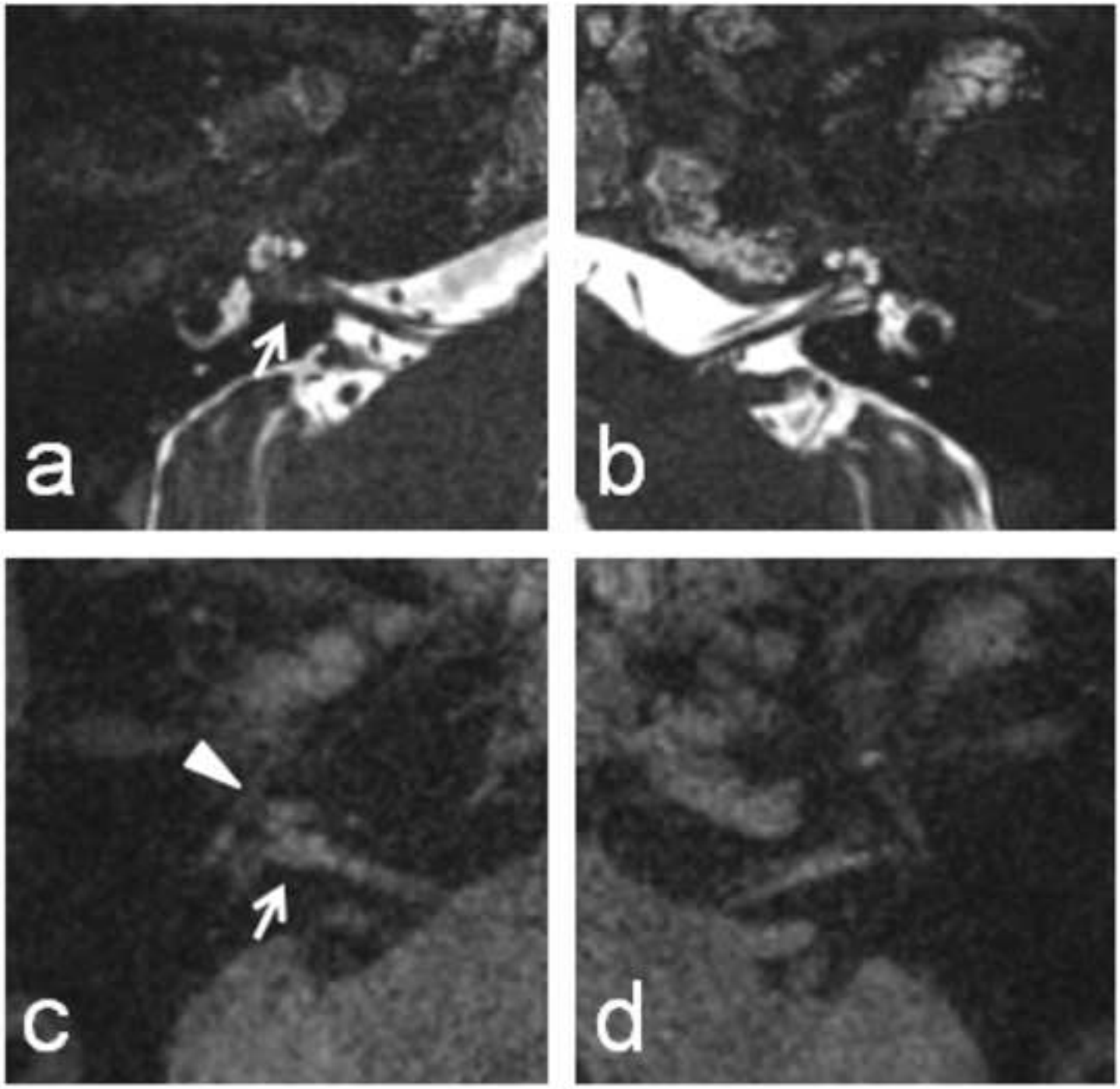

Figure 3

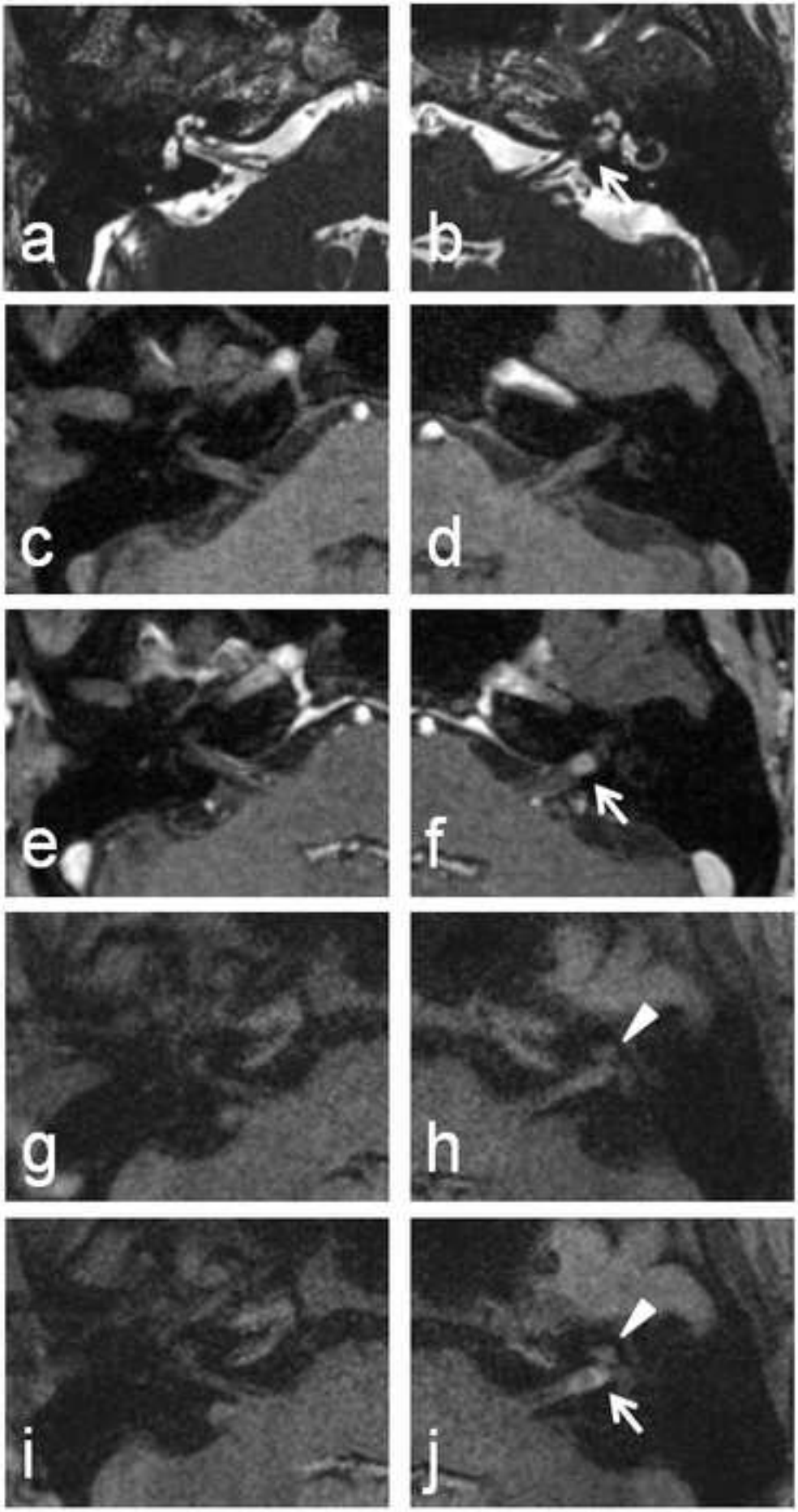

Figure 4

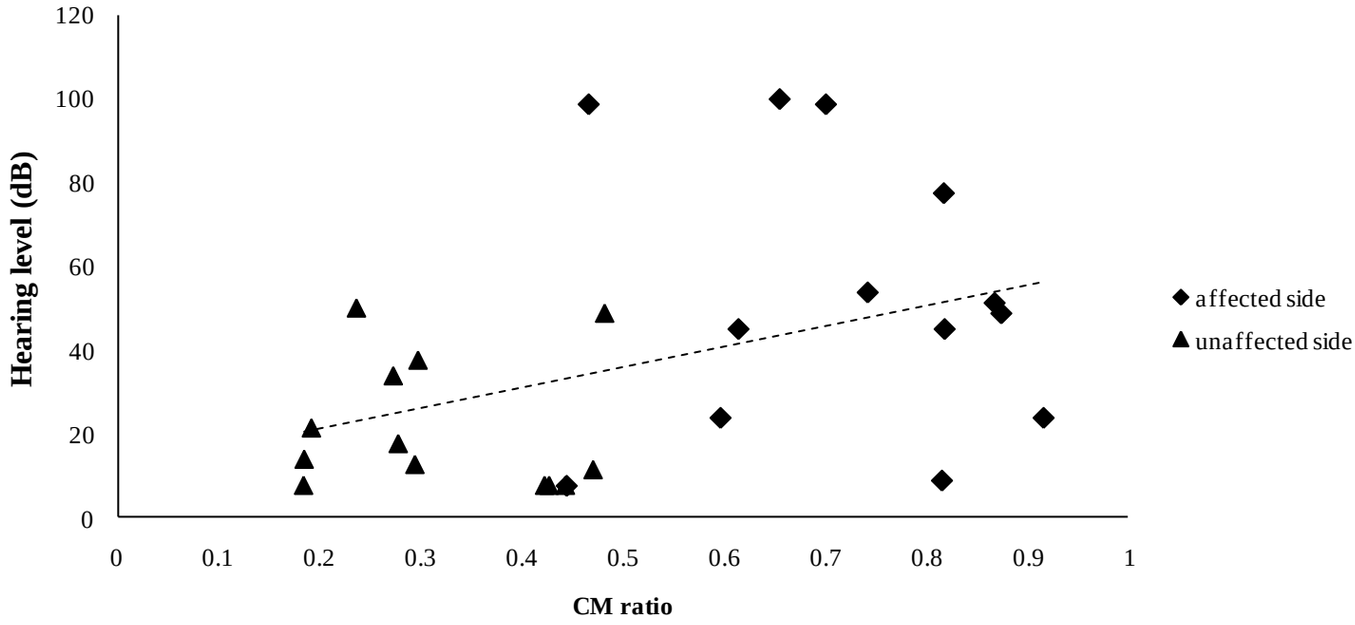
120
100
80
60
40
20
0
Hearing level (dB)
0
0.1
0.2
0.3
0.4
0.5
0.6
0.7
0.8
0.9
1
CM ratio
affected side
unaffected side